Experimental Evaluation of the Perceived Accommodation Range of a Near-Eye Light-Field Display

Jon Aschberg
Aalborg University
Medialogy
jaschb11@student.aau.dk

Anne Juhler Hansen
Aalborg University
Medialogy
ajha11@student.aau.dk

Jákup Klein
Aalborg University
Medialogy
jklein11@student.aau.dk

ABSTRACT

Near-eye Light Field Displays (NELFD) promise to alleviate several problems inherent in traditional Head-Mounted Displays (HMDs): A reduction in vergence-accommodation conflict, free accommodation within a larger range, and a significant reduction in HMD size and weight. For a reduction in vergence-accommodation conflict to be guaranteed, the accommodation range, and the depth of field within it needs to correspond approximately to realistic values. So far, these values have been estimated to correspond correctly in NELFD, but further human perception trials are needed for confirmation. We have examined the perceived accommodation range and spatial resolution in a NELFD by evaluating the performance of 30 subjects in a NELFD and actual implementation of standardized visual acuity tests, where computer generated imagery for a NELFD and real imagery were compared at several accommodation ranges. We conclude that the visual acuity (VA) score using the NELFD has high variation, but the best scores were obtained when the distance between viewer and object is below 2m. Even small incorrect physical alignment of the lens array has a negative influence on spatial resolution, and we show how small rotational and translational alignment changes can be done in software to correct for this to some degree. As of today the most limiting factor for NELFDs is the resolution, and the VA score is significantly different for reality and when using the NELFD.

1. INTRODUCTION

2D display technology is advancing at a rapid pace; both resolution and general fidelity are constantly increasing. Unfortunately, while methods for displaying 3D information have become more viable in the consumer space, these 3D systems still have severe shortcomings: Traditional 3D displays elicit what is known as the vergence-accommodation conflict wherein one has the ability to verge towards objects at different depths (change of interocular angle) without the ability to correctly accommodate (eye-lens focus).

One display technology which promises to alleviate this problem is a NELFD which utilizes microlenslets to reconstruct light rays from a scene. As the eyes verge, the light from the lenslets can form images on the retina at the correct depth and in focus. In other words, not only can the total light intensity of a ray be obtained by the viewers eye, but also the direction of each light ray.

As NELFDs are potentially a very important technology, it is vital to know exactly how the physiological and perceptual response to the displays differ from reality and traditional displays. Lanman et al. propose that with a correctly adjusted lens array and rendering output, the accommodation range of a NELFD should be able to approximate the human accommodation range, with a realistic depth of field within this range[1], but their computed model has yet to be be tested on humans for whether their model agrees with perceived values. Hiura et al. have tried to measure accommodation response in NELFDs and found there to be an approximate correlation between the response for real and NELDF distances, but more data was needed for conclusive results[2]. Perceived resolution has similarly been measured by Kovacs et al., but the results were not compared with reality[3]. Through user tests, we investigate how close the accommodation range and perceived resolution of a NELFD relate to the expected nominal values. While we are aware that the screen resolution we tested is currently one of the limiting factors, we expect that our proposed user testing methodology will still be applicable in the future.

2. RELATED WORK

2.1 The Light Field

Since space is filled with an array of light rays at various intensities, light can be interpreted as a field, and the light field describes the amount of light travelling in every direction through every point in space. The plenoptic function (from plenus, complete or full, and optic) is a 5D function that describes all light information visible from a particular viewing position[4]. In other words, the plenoptic function describes everything that can be seen as an intensity distribution: the intensity of light seen from a single viewpoint, at a point in time. This means that the plenoptic function would allow reconstruction of every possible view, from every position, at every direction, which is equivalent to a holographic representation of the visual world. Since radiance does not change along a line unless it is blocked, the 5D plenoptic function can be reduced to 4D in space free of occluders[5]. The 4D light field describes the radiance along rays (as a function of position and direction) in empty space, and explains the total amount of light intensity and the direction of each ray from the incoming light.

2.1.1 Parameterization of the 4D Light Field

Using a reduced 4D representation of the light field, Levoy et al. described how a light field can be parameterized by the position of two points on two planes, which can then be

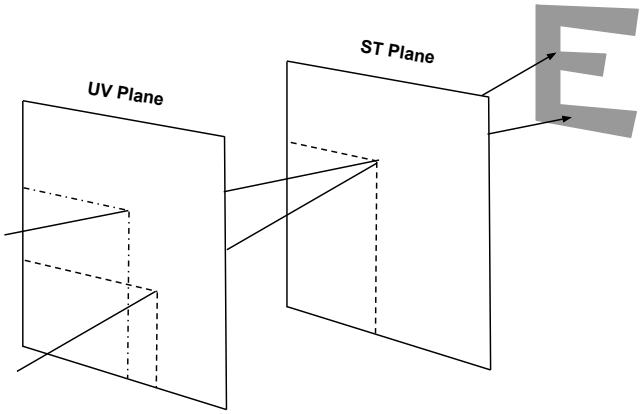

Figure 1: The light slab is a two-plane parameterization of the set of rays in a light field. The st-plane can be thought of as a collection of perspective images of the scene, while the uv-plane corresponds to the position of the observer.

actualized as a 2D array of images of a scene at different angles[5]. This parameterization is called a light slab (see Figure 1), and represents a light beam entering one plane (the uv-plane) and exiting another plane (the st-plane, which may be placed at infinity). This allows for the lines to be parameterized by two points (or a point and a direction). It has the advantage that the geometric calculations are highly efficient. A 4D light field can be represented by a 2D array of images, corresponding to images taken from different positions on the uv-plane, where each image represents a slice of the 4D light slab.

2.1.2 Capturing Light Fields and Reconstruction of 2D Images

A 2D image can be reconstructed from a light field by sampling the correct point for the specific angle and depth. This is utilized in the field of light field photography by capturing a 2D representation of the 4D light field, which can then be sampled into a 2D image with a specified depth and angle within the limits of the stored light field. In light field photography, the light field is captured either with an array of cameras[6,7], by moving a camera forward and backward[8], or by using a plenoptic camera containing an array of microlenses[9].

The reconstruction can be performed post-capture in software, where the 4D light field is computed into a 2D image. Ng et al. created the first hand-held plenoptic camera that captures the 4D light field in one photographic exposure. From this it can compute sharp photographs focused at different depths[9]. Later Georgeiv et al. created a new interpolation strategy for optimizing resolution with light field photography[10]. The interpolation method virtually increases the amount of views to be more than the amount of microlenslets and hereby creates a better resolution in the final light field photograph.

2.1.3 Optical Reconstruction

Instead of reconstructing 2D images in software, the same effect can be achieved optically by placing a distance-adjusted array of microlenses in front of a representation of a light field by an array of 2D images (see Figure 2). This allows for an observer at the correct distance to integrate a correct 2D image of the light field at different depths and angles in accordance with the spatial and depth resolution that the light field contains. This is known as a light field display. By using concepts from integral imaging displays and light field photography, Lanman and Luebke recently introduced a light field display optimized for near eye viewing[11].

2.2 Head-Mounted Light Field Displays

There are several benefits from using microlenslet arrays in head-mounted displays (HMD). Lanman et al. have shown that a light field display can be integrated into an HMD, which can potentially allow for much more immersive VR solutions compared to the fixed focus displays used in most common HMDs[11]. Shaulov et al. demonstrated that ultra-compact imaging optical relay systems based on microlenslet arrays can be designed with an overall thickness of only a few millimeters[12], and near-eye light field displays have been created with a thickness of 1 cm.[1]

Head-Mounted Displays as of writing are still struggling with being heavy and having bulky optics[13]. Most HMDs do not account for the vergence-accommodation conflict (see Section 2.3.1), and they suffer from low field-of-view (FOV) and low resolution. Since light fields consist of more information than usual 2D images, light fields can improve on some of the limitations of traditional fixed-focus HMDs.

2.3 Visual Perception

As the eyes of a human look at features at different distances, the ocular system tries to adapt its parameters such that the point of interest remains binocularly fused and in focus. Two of these parameters are vergence and accommodation. When accommodating to a certain distance, the shape of the lens inside the eye changes to allow for a focused image at that distance plane, with surrounding distances in varying states of focus. Humans can change the optical accommodation of their eyes by up to 15 diopters (the inverse of the focal length in meters), falling off with age[14].

The second distance mechanism continually adjusts the angle between the two eyes such that features at the focus distance remain fused in the binocular vision. This effect is known as vergence. As the distance of the point of interest decreases from infinity, the pair of eyes will converge along their vertical axis, or on the other hand, they will divergence when looking further away from a point. Both systems are driven by the logical cues relating to their area: retinal blur prompts an oculomotor accommodation adjustment, and stereo disparity drives the eyes to converge or diverge. Unfortunately for stereographic systems, there is a secondary set of cues for both systems consisting of reciprocal signals from one another; a feedback loop for both systems. Suryakumar et al. have shown that visual disparity in isolation elicits a fully comparable accommodation response to that of retinal blur[15], strengthening the argument that these systems are very tightly coupled.

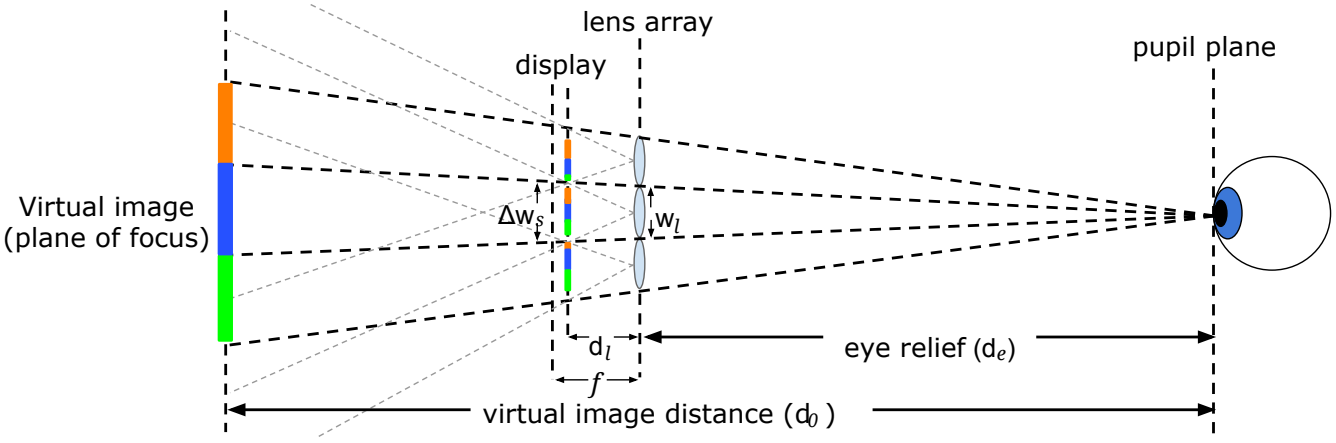

Figure 2: The Near-Eye Light Field Display; a microlens array is placed in front of the display and the human eye optically reconstructs the virtual image from the rendered 2D light field image

2.3.1 *Vergence-Accommodation Conflict*

In natural viewing conditions the reciprocal secondary cues between accommodation and vergence serve to better coordinate the final accommodative response[16]. However, in traditional stereo imaging where the depth is fixed, vergence towards a different distance will elicit irreconcilable cues between the two systems. This signal conflict has been linked to discomfort[17], visual fatigue, and reduced visual performance[18]. Research in resolving this conflict is still ongoing, with several proposals across the spectrum between hardware and software[19].

One of the intrinsic benefits of light field displays is that they allow for natural accommodation within a range of depths. Adjusting the parameters described in Section 2.1.3, the optically reconstructed image can be rendered to be perceived as if they are at natural (or unnatural) distances away from the viewer. Accommodation towards differing distances determines which image slices are focused onto the retina.

2.3.2 *Perceived Resolution and Visual Acuity*

With a light field display, the final image that reaches the retina is the combination of light from hundreds of different views, as such, the term "resolution" for a light field display is hard to accurately describe. The resolution of each individual view does not necessarily correspond to the perceived resolution. Kovács et al. did a study to determine the perceived resolution of 3D light-field displays. They chose a subjective model and compared with objective methods. They argue that the subjective method is necessary due to the fact that there is no standardized way of measuring resolution of light field displays[3]. They used "tumbling E's" for the subjective model. This method is similar to existing visual acuity tests.

Visual acuity (VA) is a measure of the acuteness of vision or in other words the spatial resolution in the visual processing system. Visual acuity tests have been developed since the 1860s, with the Snellen Chart being one of the most famous ones, that also advocated the need for a standardized vision test[20].

We propose that the perceived resolution of the light field display at different accommodation distances can be examined by comparing subjects' real-life VA to their VA while using the NELFD and analyzing the difference. The VA scores recorded for participants while using the NELFD are not indicative of the participants' actual VA, but a way to analyze the degradation in performance that is likely to exist owing to the comparatively low resolution of the microdisplay.

2.3.3 *Measuring Accommodation Response*

There has been some work investigating the effectiveness of light field displays as far as accommodation is concerned. Huira et al. measured the accommodation response of users with an autorefractor[2]. The users were placed in front of an integral display with an autorefractor between. The stimulus was a 3D object shown in 1 cm intervals. In addition to the measurements with the autorefractor, the users were asked what they thought the distance to the 3D object was. The authors concluded that there was an approximate correlation between the perceived distance and the accommodation response. As of the time of testing, an autorefractor was not available to us, and our method for measuring response consists of test participants being subjected to several visual acuity charts at varying accommodation distances, and their performance delta from a non-NELFD chart is analyzed. Distances that can be accommodated towards would then score higher, and scores would fall off outside.

2.3.4 *Measuring Perceived Resolution*

In 1982 Ferris et al. suggested a new chart for evaluating visual acuity. The then current charts (e.g. Snellen chart) had unregular progression in letter size and uneven number of letters in every line. They introduced the LogMAR ETDRS (from now on referred to as LogMAR) chart as a solution to these problems[21]. LogMAR has since become the gold standard for visual acuity measurement[22]. One problem with the LogMAR chart is that it requires a long time to complete. To alleviate this, the reduced LogMAR was created and thereby features the advantages of the LogMAR chart, but requires less time to complete due to its smaller size.[22].

Bourne et al. suggested to replace the letters on the reduced LogMAR chart with "tumbling E" optotypes (optotypes are

the symbols used in vision charts), and called it the reduced LogMAR E-chart (RLME). Four possible "letters" can be achieved by rotating the optotype in randomized 90° intervals. The chart was designed for subjects not familiar with the roman alphabet, and instead the test participants would point in the orientation of the optotype[23]. This chart can also be used for gaining more automation in the test procedure, where instead of pointing in the orientation of the optotype the participants would move a joystick. This would allow for easy logging of the users performance, which is measured using the "single-letter" score.[23] Equation 1 shows how the score is calculated where T_c is the total number of correct responses, and L_v is the LogMAR value of each letter.

$$\text{LogMARscore} = 1.10 - T_c L_v \tag{1}$$

3. IMPLEMENTATION AND METHODS

The NELFD is constructed using an array of lenses (a Fresnel Technologies #630 microlens array) in front of an array of rendered images on a microdisplay (see Figure 2 for a general overview). Each of the lenslets in the lens array works as a simple magnifier for each of the elemental images in the array. The alignment of the lenses is influenced by several parameters and especially the lens separation d_l has great impact on the perceived image. The lens separation can be found using the Gaussian thin lens formula (see Equation 2), where d_l is the distance between the lens and the display, f is the focal length, d_0 is the distance to the virtual image, and d_e is the eye relief.

$$\frac{1}{f} = \frac{1}{d_l} - \frac{1}{d_0 - d_e} \Leftrightarrow d_l = \frac{d_0 - d_e}{f + (d_0 - d_e)} \tag{2}$$

The microlens array should be placed at a distance $0 < d_l \leq f$, and we can see from the Gaussian thin lens formula that with an eye relief of 15mm and d_0 set to 1 meter, then the lens separation should be 3.29mm or in other words just below the focal length $f = 3.3$ mm. The lens separation was manually adjusted to the best possible alignment ≈3.29mm.

The magnification factor is M=299.48 (see Equation 3), where w_0 is the width of the virtual image at the plane of focus, and w_s is the width of the microdisplay. The magnification factor tells us the magnification of the image on the screen to the image plane at d_0, and is used to calculate the field of view.

$$M = \frac{w_0}{w_s} = \frac{d_0 - d_e}{d_l} = 1 + \left(\frac{d_0 - d_e}{f}\right) \tag{3}$$

Through the Unity engine[24], a virtual image is rendered for every lenslet that is completely within the bounds of the microdisplay. After the physical alignment of the lenses, pixels can be sacrificed for final small-scale rotational and translational software alignment.

The FOV is limited either by the extent of the lens (lens-limited magnifier is influenced by $\frac{w_l}{2d_e}$) or it is limited by the dimensions of the display (display-limited magnifier is influenced by $\frac{Mw_s}{2d_0}$). In this case the FOV can only be limited by the lens (see Equation 4). The FOV per rendered camera is then 17.28°.

$$\alpha = 2 \arctan\left(\frac{w_l}{2d_l}\right) \tag{4}$$

Since a microlens array can be interpreted as a set of independent lens-limited magnifiers, the total field of view from the viewers eye can be found by substituting the lens separation d_l with the eye relief d_e, and the lens width w_l with the array width $N_l w_l$. The total FOV α_t is then given by Equation 5, where N_l is the number of lenses. The vertical FOV for 14 lenses is $FOV_v = 50.03°$ and the horizontal FOV for 8 lenses is $FOV_h = 29.86°$ (see Equation 5).

$$\alpha_t = 2 \arctan\left(\frac{N_l w_l}{2d_e}\right) \tag{5}$$

$$N_p = \left(\frac{2d_0 \tan(\alpha/2)}{Mp}\right) \tag{6}$$

With respectively $FOV_v = 50.03°$ and $FOV_h = 29.86°$ we get a resolution of 157x90 px (see Equation 6). The FOV α is expanded by the number of lenses N_l, but since part of the rendered image is repeated across some or all of the elemental images, this repetition reduces the perceived spatial resolution.

When a point is in perfect focus a corresponding point is on the image plane. If the point is not on the focus plane the point will form a circle due to the light not converging on the image plane but rather in front or behind. This is called the circle of confusion. Due to the circle of confusion the only section of a scene being in focus is the focus plane. However as a point approaches the focus plane the size of the circle of confusion decreases approaching zero. This means that any circle of confusion below the lowest level of detail that the system is able to distinguish appears to be in focus. In the case of a screen the smallest distinguishable detail is the pixel, so if the circle of confusion is equal or smaller than one pixel, the point can not appear more in focus.

The circle of confusion c_0' is therefore dependent on the optical characteristics that determine how the size of the circle of confusion changes over distance d_0'. Additionally the circle of confusion depends on the screen since the circle can not be smaller than a single pixel (see Equation 7, where p is the pixel pitch.) Note that the circle of confusion being calculated is not the circle of confusion on the image plane but rather on the focus plane.

$$c_0' = \max\left(\left(\frac{d_0' - d_0}{d_0 - d_e}\right) w_l, \left(\frac{d_0' - d_e}{d_l}\right) p\right) \tag{7}$$

The depth of field is the area surrounding the focus point that appears to be in focus due the the circle of confusion being smaller that the smallest distinguishable detail (pixel pitch p). Figure 3 shows the two factors in the circle of confusion:

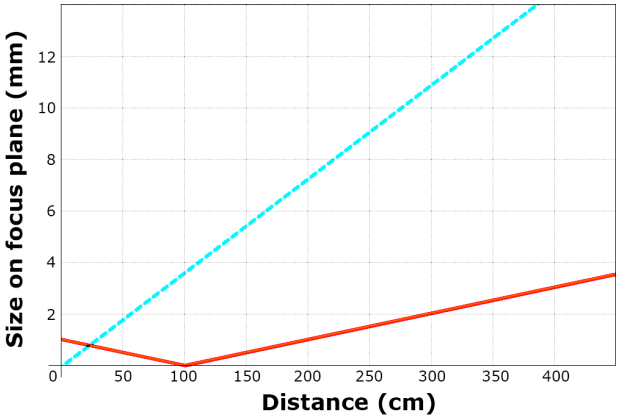

Figure 3: Graph of both elements from Equation 7 showing the two factors defining the circle of confusion. The red line shows the actual circle of confusion while the dotted cyan line shows the smallest detail that is possible to show.

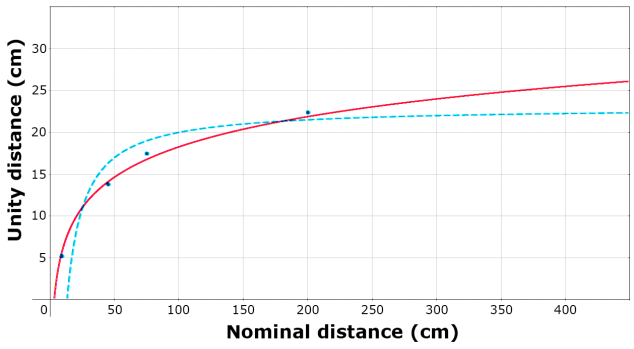

Figure 4: Graph showing the two proposed curves (red: see Equation 8, cyan: see Equation 9) for converting real distances to the equivalent virtual distances. Also shown are the points the curves are fitted to, one additional measurement was made at optical infinity that is not shown on the graph (the Unity distance had not changed from the previous measurement at 200cm).

actual circle of confusion from the lens, and the smallest detail possible due to pixel pitch. As long as the optical circle of confusion is smaller than a pixel the point appears to be in focus. In our setup the depth of field stretches from 22.9cm and continues to infinity.

Each elemental image is rendered from a virtual camera to a portion of the microdisplay (optimally 15mm × 8mm out of 15.36mm × 8.64mm), with less available depending on how much lens alignment is done in software instead of physically. Software alignment is thus ideally only used for small-scale adjustments to achieve higher spatial resolution with slight physical misalignment. The size of the elemental images should be the same at the size of the lenslet (1mm × 1mm) with the center of the elemental image corresponding to the center of the lenslet.

The virtual camera array forms a grid that would ideally be spaced with the same distance as that between each lenslet (1mm), but any spacing is usable, as long as the relationship follows the physical lens-spacing in both axes. Scaling the grid spacing essentially scales the virtual world size accordingly. For our NELFD we increase this grid by a factor of 1000 to move the world further away from the nearest possible camera clipping plane for our rendering engine (object distances are adjusted accordingly), and use the previously calculated FOV for each camera (see Equation 4).

Initially, the relationship between distances in the simulation and reality were found to not be in accord, likely due to inaccuracies in physical alignment and distance estimation. To correctly map the virtual and physical distances, a camera (aperture size $f/1.8$) was manually focused at several distances. With the camera lens only capable of focusing within the range of 45cm to optical infinity, closer distances were estimated based on human comparisons of nearest focal distance for reality and the NELFD. With these measurements, the relationship to the linear in-engine distance was mapped to the function that best coincided with all the physically measured distances (see Equation 8). A reciprocal function (see Equation 9) is potentially as likely to fit the data-points (see Figure 4).

$$f(x) = log\left(\frac{x}{3}\right) \times 12 \tag{8}$$

$$f(x) = -\left(\frac{1}{x}\right) \times 300 + 23 \tag{9}$$

4. EXPERIMENT

The experiment took place at small room where the participants were seated 2 meters from a computer screen. The screen showed an image of a randomized RLME chart where the optotypes on the top line were 5 arc-minutes high (2.909 cm at 2 meters distance). The input device was a Xbox 360 controller. The test participants used buttons on the Xbox controller to indicate how they believed the "E"s were oriented. Additional buttons were used go back to previous optotypes in case the test participants thought they made a mistake.

The RLME charts were randomly generated inside blocked distance ranges (see Table 1).

	Center	Lower	Upper	Beyond
Center	100	10-100	100-500	-
Lower	10-100	-	10-500	-
Upper	100-500	10-500	-	500-5000
Beyond	-	-	500-5000	-

Table 1: Matrix of accommodation ranges in cm wherein samples are taken.

The experiment started with the participant signing a consent form. They were then seated 2 meters from a computer screen showing a visual acuity chart. They were then given the NELFD and were given 5 similar acuity tests at different

distances (see Table 1 for a list of the ranges). They used the Xbox controller to answer all tests. The test participants were asked to give their best answer even when they no longer could see the optotypes.

4.1 Results

A total of 30 test subjects participated in the experiment (27 male, 3 female). 27 participants were students, and 3 were either employed or unemployed. 6 had no previous experience with HMDs, 12 had tried it a few times, and 11 were experienced users. 22 answered that they have normal sight, 8 answered no to having normal sight. 2 of the test participants use glasses and 7 use contact lenses. 7 of the test participants use their glasses/contact lenses all the time, and the rest for reading or the like. Invalid scores and test participants using glasses were excluded from the results.

The collected data consist of continuous ratio input variables (distance from chart to viewer) and discrete interval level response variables (LogMAR scores).

As expected there is a significant difference between the LogMAR scores in reality and the LogMAR scores using the NELFD ($p = 2.2852 \times 10^{-16}$ for $\alpha = 0.05$ using the Wilcoxon rank sum test). This indicates that the test participants' VA LogMAR scores are lower when using the NELFD (mean: 0.6654 LogMAR) compared to their VA LogMAR scores in reality (mean: -0.1124 LogMAR). Said in other words: the test participants VA is better in reality than using the NELFD.

The LogMAR scores using the NELFD has a range from $0.1343 - 0.8669$ LogMAR (mean: 0.6654 LogMAR) for varying distances between 10 cm to 50 m. Due to the generally large variance in the LogMAR scores across distances (see Figure 5) meaningful analysis is hard. If however the data is organized according to LogMAR score rather than distance it becomes apparent that while high LogMAR scores (low visual acuity) spans across all distances the low scores (high visual acuity) is limited to distances under 1m (see Figure 6). This is only the case when outlier are not taken into account.

Estimating the correlation through Spearman's RHO reveals that the distance and the LogMAR score is positively ($r = 0.4321$) correlated (p=1.6612×10^{-7} for $\alpha = 0.05$). This means that as the distance increases, so does the LogMAR score, which is equivalent to a lower VA performance).

Likewise the ΔLogMAR score (the difference in VA LogMAR score in reality and using the NELFD) is positively ($r = 0.2345$) correlated (p=0.0062 for $\alpha = 0.05$). So when the distance increases the more the test participants VA LogMAR score will increase away from their LogMAR scores in reality (meaning the difference will get bigger, as the test participants VA performance is decreasing).

5. CONCLUSION AND DISCUSSION

The results indicate that there is a significant difference in visual acuity (VA) performance between the Near-Eye Light Field Display (NELFD) and real life. The difference would likely be lower with a higher resolution NELFD.

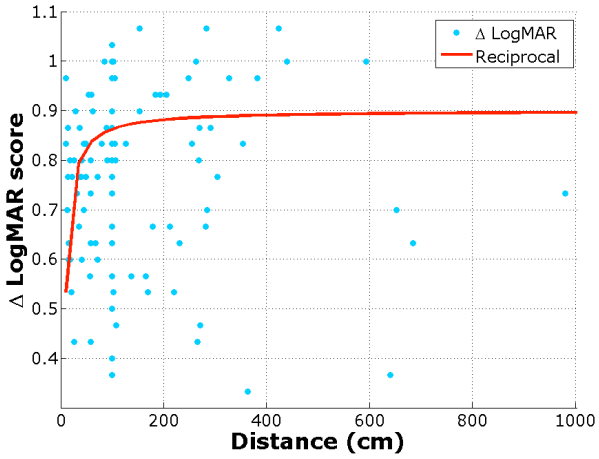

Figure 5: Delta LogMAR score over virtual distance (cm)

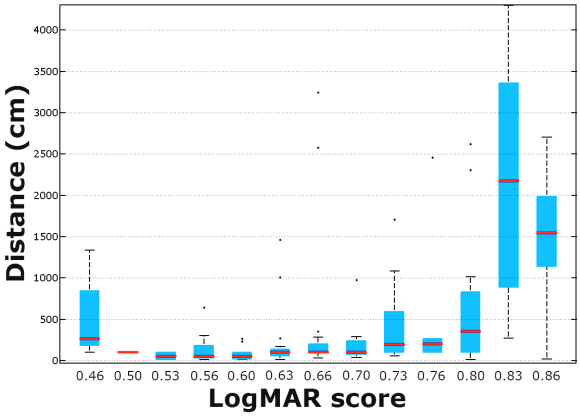

Figure 6: Lower variance in virtual distance for better VA

We conclude, that there is positive correlation between the VA and the distance to the chart in the NELFD: As the distance increases the test participants' VA is reduced.

We estimate that our NELFD should have an accommodation range spanning 22.9cm to optical infinity, and while this appears to be the case, observations and camera measurements finds optical infinity to be reached at 2m, and objects at further distances have increasingly lower spatial resolution. VA results corroborate this finding: LogMAR performance decreases with distance. It therefore appears that there is a reduction in VA where the rendered images should be tending towards complete uniformity as the virtual distance to the chart approach infinity. Distances towards in-engine infinity are thus in practice beyond optical infinity for the observer and cannot be focused. We speculate that the light rays from a meaningful amount of elemental images are parallel to the observer before the point where the renders are actually parallel. Therefore, moving beyond the point where the rays are parallel to the observer, the rays diverge in the wrong direction and nothing can be fully in

focus without additional optics. We further speculate that these results are due to misalignment between the elemental images and the lenslets.

The Δ LogMAR score (difference in VA LogMAR score between reality and in the NELFD) was calculated for all test participants, and here there was a positive correlation between Δ VA and distance. As the distance increases, the VA of the test participants in the NELFD increasingly differ from their VA score in reality.

We conclude that the NELFD technology works. The VA results for participants using the NELFD have too high a variance to draw statistically significant conclusions from, but do seem to have the best LogMAR scores where the distance between viewer and chart is within a few meters. Correct physical alignment is essential to approach the optimal spatial resolution for the NELFD, though small alignment changes can be done in software. As of writing, the most limiting factor for NELFDs is the pixel density of the display, and we encourage further studies in the field of NELFD in the future, when higher resolution microdisplays become available.

5.1 Future work

The lenses have to be aligned to the elemental images perfectly. In our case this was not possible with the equipment available, and software alignment invariably results in underutilized pixels. The software translation rotation of the elemental images resulted in a quite good alignment, but it was not perfect. The alignment might have become better if the possibility of scaling the elemental images had also been investigated (especially for larger accommodation distances).

In this project only monocular vision was tested, in a future revision stereo vision should be investigated.

References

[1] Douglas Lanman and David Luebke. Supplementary material: Near-eye light field displays. *ACM Transactions on Graphics (TOG)*, 32(6):220, 2013.

[2] Hitoshi Hiura, S Yano, T Mishina, J Arai, K Hisatomi, Y Iwadate, and T Ito. A study on accommodation response and depth perception in viewing integral photography. *Proc. 3DSA*, pages P2–2, 2013.

[3] Peter Tamas Kovacs, Kristof Lackner, Attila Barsi, Akos Balazs, Atanas Boev, Robert Bregovic, and Atanas Gotchev. Measurement of perceived spatial resolution in 3d light-field displays. In *Image Processing (ICIP), 2014 IEEE International Conference on*, pages 768–772. IEEE, 2014.

[4] Edward H Adelson and James R Bergen. The plenoptic function and the elements of early vision. *Computational models of visual processing*, 1(2):3–20, 1991.

[5] Marc Levoy and Pat Hanrahan. Light field rendering. In *Proceedings of the 23rd annual conference on Computer graphics and interactive techniques*, pages 31–42. ACM, 1996.

[6] Bennett S Wilburn, Michal Smulski, Hsiao-Heng K Lee, and Mark A Horowitz. Light field video camera. In *Electronic Imaging 2002*, pages 29–36. International Society for Optics and Photonics, 2001.

[7] Hartmut Schirmacher, Li Ming, and Hans-Peter Seidel. On-the-fly processing of generalized lumigraphs. In *Computer Graphics Forum*, volume 20, pages 165–174. Wiley Online Library, 2001.

[8] Cha Zhang and Tsuhan Chen. Light field capturing with lensless cameras. In *Image Processing, 2005. ICIP 2005. IEEE International Conference on*, volume 3, pages III–792. IEEE, 2005.

[9] Ren Ng, Marc Levoy, Mathieu Brédif, Gene Duval, Mark Horowitz, and Pat Hanrahan. Light field photography with a hand-held plenoptic camera. *Computer Science Technical Report CSTR*, 2(11), 2005.

[10] Todor Georgiev, Ke Colin Zheng, Brian Curless, David Salesin, Shree Nayar, and Chintan Intwala. Spatio-angular resolution tradeoffs in integral photography. *Rendering Techniques*, 2006:263–272, 2006.

[11] Douglas Lanman and David Luebke. Near-eye light field displays. *ACM Transactions on Graphics (TOG)*, 32(6): 220, 2013.

[12] Vesselin Shaoulov, Ricardo Martins, and Jannick P Rolland. Compact microlenslet-array-based magnifier. *Optics Letters*, 29(7):709–711, 2004.

[13] JP Rolland and Hong Hua. Head-mounted display systems. *Encyclopedia of optical engineering*, pages 1–13, 2005.

[14] W Neil Charman. The eye in focus: accommodation and presbyopia. *Clinical and experimental optometry*, 91(3):207–225, 2008.

[15] Rajaraman Suryakumar, Jason P Meyers, Elizabeth L Irving, and William R Bobier. Vergence accommodation and monocular closed loop blur accommodation have similar dynamic characteristics. *Vision research*, 47(3): 327–337, 2007.

[16] Clifton M Schor, Jack Alexander, Lawrence Cormack, and Scott Stevenson. Negative feedback control model of proximal convergence and accommodation. *Ophthalmic and Physiological Optics*, 12(3):307–318, 1992.

[17] Takashi Shibata, Joohwan Kim, David M Hoffman, and Martin S Banks. Visual discomfort with stereo displays: Effects of viewing distance and direction of vergence-accommodation conflict. In *IS&T/SPIE Electronic Imaging*, pages 78630P–78630P. International Society for Optics and Photonics, 2011.

[18] David M Hoffman, Ahna R Girshick, Kurt Akeley, and Martin S Banks. Vergence–accommodation conflicts hinder visual performance and cause visual fatigue. *Journal of vision*, 8(3):33, 2008.

[19] Gregory Kramida and Amitabh Varshney. Resolving the vergence-accommodation conflict in head mounted displays.

[20] Herman Snellen. *Dr. H. Snellen's Probebuchstaben zur Bestimmung der Sehschaerfe*. H. Peters, 1863.

[21] Frederick L Ferris, Aaron Kassoff, George H Bresnick, and Ian Bailey. New visual acuity charts for clinical research. *American journal of ophthalmology*, 94(1): 91–96, 1982.

[22] DA Rosser, DAH Laidlaw, and IE Murdoch. The development of a "reduced logmar" visual acuity chart for use in routine clinical practice. *British Journal of Ophthalmology*, 85(4):432–436, 2001.

[23] RRA Bourne, DA Rosser, P Sukudom, B Dineen, DAH Laidlaw, GJ Johnson, and IE Murdoch. Evaluating a new logmar chart designed to improve visual acuity assessment in population-based surveys. *Eye*, 17(6): 754–758, 2003.

[24] http://unity3d.com/5?gclid=CObkm4rW4MUCFYUMcwod4C0ACg. Accessed May 27, 2015.